International Journal of Statistics and Applied Mathematics

**ISSN:** 2456-1452
Maths 2023; 8(2): 117-123
© 2023 Stats & Maths
https://www.mathsjournal.com
Received: 25-01-2023
Accepted: 29-02-2023

**Maibam Sanju Meetei**
Associate Professor,
Department of Electronics and Communication Engineering,
Rajiv Gandhi University,
Doimukh, Arunachal Pradesh,
India

**Corresponding Author:**
**Maibam Sanju Meetei**
Associate Professor,
Department of Electronics and Communication Engineering,
Rajiv Gandhi University,
Doimukh, Arunachal Pradesh,
India

# Modelling and simulation of TMCPS using PMMA

**Maibam Sanju Meetei**

**DOI:** https://doi.org/10.22271/maths.2023.v8.i2b.968

**Abstract**
In this paper, a mathematical modeling of the Touch Mode Capacitive Pressure Sensor (TMCPS) is presented and validated by using the COMSOL Multiphysics simulator. The output characteristic of TMCPS is linearized and thereby achieved by using a mechanical coupler which is utilized to convert the deflection of the diaphragm due to applied pressure into a linear displacement. A square diaphragm is designed for conversion of pressure into displacement to calculate the maximum deflection of the square diaphragm and the output capacitance of the sensor. A 3D model of the design sensor is built and simulated using a COMSOL Multiphysics simulator to compare the calculated values and simulated output values. The various factors affecting the sensitivity of TMCPS: the physical parameters of the diaphragm, mechanical properties (Poisson's ratio &Young modulus), permittivity of the polymer, physical parameters of the capacitor plates, and gap between the capacitor plates are considered to validate the values. The sensitivities of the Poly-Methyl Methacrylate (PMMA) based TMCPS with a diaphragm thickness of 20 µm for simulated and calculated are found as 0.035fF/MPa and 0.034 fF/MPa respectively.

**Keywords:** Capacitance, mechanical coupler, permittivity, sensitivity, touch mode

## 1. Introduction
The There are various types of pressure sensor based on their sensing mechanism. They are based on resistive, capacitive, inductive, thermal, piezoelectric, optical etc [1-6]. The piezoelectric and resistive pressure sensors are also wide used in MEMS application as they can also be miniaturized [7-9]. Among these based sensors capacitive based pressure is used in broad range because it can sense high pressure, low power consumption and can be miniaturized [10-11]. The basic classifications of capacitive pressure sensor based on their structures are conventional planar capacitive pressure sensor, touch mode capacitive pressure sensor and comb structure capacitive pressure sensor [12-13]. The conventional planar capacitive pressure sensor has a diaphragm plate and a based plate. In diaphragm plate, the pressure is applied and changes in capacitance between the diaphragm plate and the based plate are measured as an output and this output is nonlinear with the applied pressure. TMCPS has similar structure with conventional planar capacitive pressure sensor but dielectric materials are placed on the based plate and touched by the diaphragm plate when it is deflected due to the applied pressure. The output of TMCPS is nonlinear but they have higher sensitivity than the conventional planar type capacitive pressure sensor. The comb structure capacitive pressure sensor has inter-digited finger of the comb which increases the surface area leading to increase in the output capacitance. The output capacitance of this sensor is nearly linear to the applied pressure. Among these sensors, TMCPS is very promising and it can be operated in wide range of high pressure and higher sensitivity.

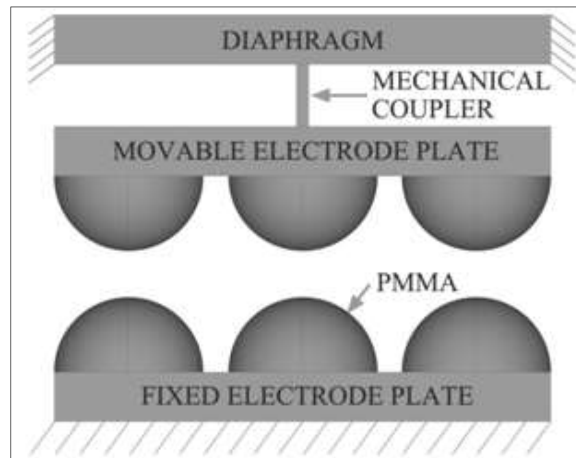


**Fig 1:** Side view of TMCPS with a Mechanical Coupler.

In this study a modified TMCPS as shown in figure 1 with a mechanical coupler is carried out. The modified TMPCS has a mechanical coupler connected with diaphragm in one end and movable electrode plate at the other end. Hemisphere polymers dielectrics are attached with the movable electrode plate and the fixed electrode plate. The pressure is applied at the diaphragm and a maximum deflection occurs at the center of the diaphragm. With the help of the mechanical coupler this deflection is converted into linear displacement. The movable electrode plate moves and changes in capacitance which is directly proportional to the applied pressure. This polymer dielectric keeps away the touching of movable electrode plate and fixed electrode plate.

## 2. Design Method

It is necessary to design a mathematical model of the sensor to find out the various parameters affecting the output of the sensor. Then to verify the calculated values, simulations of the model sensor are done and compared with the output and simulated values.

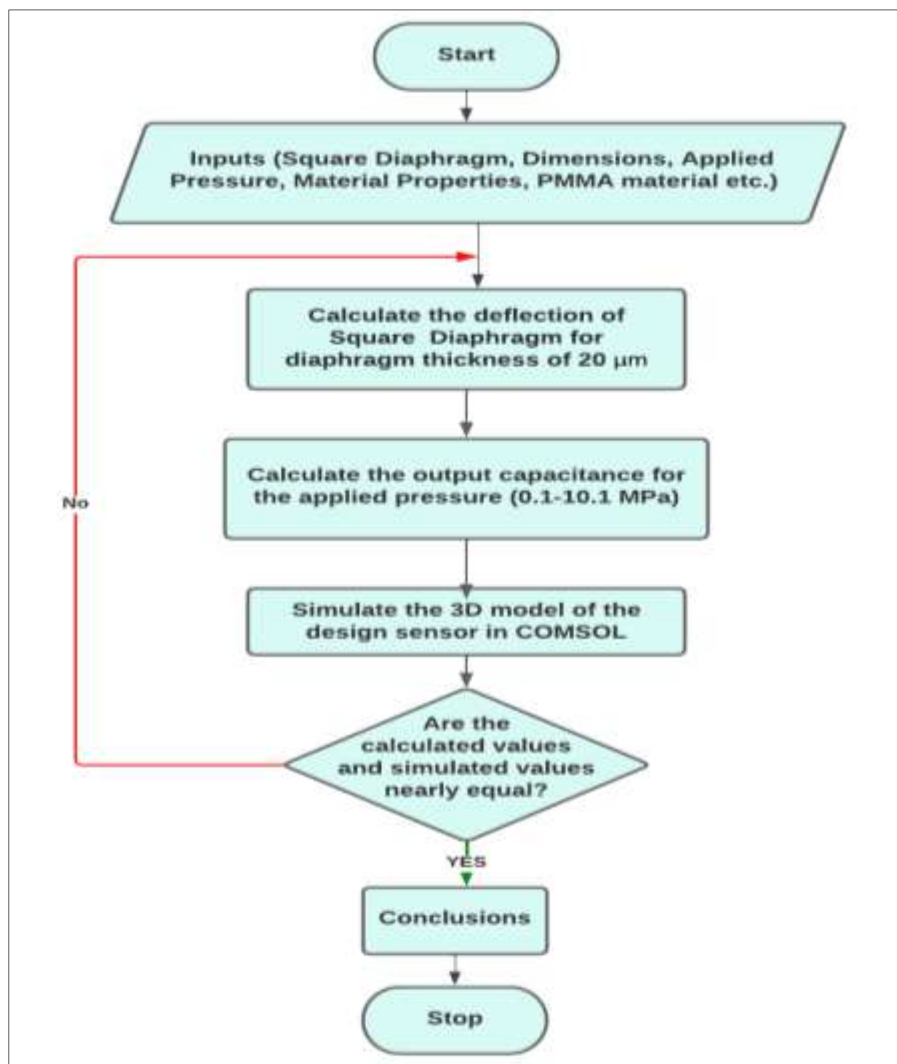


**Fig 2:** Flowchart of the design methodology.

The mathematical model of the sensor has two parts, mechanical and electrostatic as the pressure sensor converts the mechanical displacement due to applied pressure into output voltage. The design flow of this research work is shown in figure 2.
The mechanical coupler transforms the diaphragm's deflection into a linear displacement on the movable electrode plate. The linear displacement causes the moveable electrode plate closer to the fixed electrode plate, changing the capacitance output of the sensor. The variation in output capacitance is directly proportional to the applied pressure.

### 2.1 Mechanical Modelling

The square diaphragm and circular diaphragm are the most commonly used diaphragms in sensors. In our study a square diaphragm is considered because it has a higher deflection than the circular diaphragm for the same applied pressure. Let us consider first a rectangular diaphragm of length 2b along the y-axis and breadth 2a along the x-axis. To calculate the total energy H of the diaphragm under applied pressure P is as follow [14-16].

$$H = \frac{D}{2}\int_{-b}^{b}\int_{-a}^{a}\left\{\left(\frac{\partial^2\zeta(x,y)}{\partial x^2} + \frac{\partial^2\zeta(x,y)}{\partial y^2}\right)^2 - 2(1-v)\left\{\frac{\partial^2\zeta(x,y)}{\partial x^2}\frac{\partial^2\zeta(x,y)}{\partial y^2} - \left(\frac{\partial^2\zeta(x,y)}{\partial x\partial y}\right)^2\right\}\right\}dxdy - \int_{-b}^{b}\int_{-a}^{a}\zeta(x,y)Pdxdy, \quad (1)$$

where, ζ(x, y) is the deflection function, D is the flexural rigidity and v is the Poisson's Ratio. The value of flexural rigidity is provided by

$$D = \frac{Et^3}{12(1-v^2)}. \quad (2)$$

where, t is the thickness of the diaphragm and E is the Young's Modulus of the diaphragm material.
The deflection function ζ(x, y) of a rectangular diaphragm is given by [15-16].

$$\zeta(x,y) = \omega(a^2 - x^2)^2(b^2 - y^2)^2, \quad (3)$$

Where, ω is a constant. Now, substituting equation 3 with equation 1 and applying the condition, we get

$$\omega = \frac{49P}{128(7a^4+4a^2b^2+7b^4)D}. \quad (4)$$

By substituting equation 4 into equation 3, we get

$$\zeta(x,y) = \frac{49P}{128D(7a^4+4a^2b^2+7b^4)}(a^2 - x^2)^2(b^2 - y^2)^2. \quad (5)$$

For a square diaphragm, the length of the all sides are equal i.e. *a*=*b*, then equation 5 becomes

$$\zeta(x,y) = \frac{49P}{128D(7a^4+4a^2a^2+7a^4)}(a^2 - x^2)^2(a^2 - y^2)^2,$$

$$.\ \zeta(x,y) = 0.02126\frac{Pa^4}{D}\left(1 - \frac{x^2}{a^2}\right)^2\left(1 - \frac{y^2}{a^2}\right)^2. \quad (6)$$

Equation (6) is the function of deflection of a square diaphragm at any given coordinates. The maximum deflection occurs at the centre of the diaphragm i.e. (*x, y*)=(0,0), now the maximum deflection of a square diaphragm is given by

$$\zeta(x,y)\frac{Pa^4}{D}_{max}. \quad (7)$$

The flexural rigidity, length of the side, and applied pressures are the parameters that affect the maximum deflection of the square diaphragm.

### 2.2 Electrostatic Modelling

A design model of the TMCPS with PMMA polymer dielectric is shown in figure 1. The electrode plates are partially coated with hemispherical polymers and some are not coated. The areas of the electrodes are divided into two areas, one area is the area covered by the dielectric polymers and another area is the area not covered by dielectric polymers. Therefore, the overall capacitance $C$ can be calculated by the sum of capacitances $C_1$ and $C_2$. Where $C_1$ is the capacitance of the area covered by the dielectric polymers and $C_2$ is the capacitance of the area not covered by the dielectric polymers.

$$C = C_1 + C_2, \quad (8)$$

Now, $C_1$ and $C_2$ can be expressed as

$$C_1 = n\frac{\varepsilon_0\varepsilon_r}{(g-\zeta)}\pi r^2, \tag{9}$$

$$C_2 = \frac{\varepsilon_0(\theta - n\pi r^2)}{(g-\zeta)}, \tag{10}$$

where $n$ is the number of hemispherical dielectric attached to an electrode plate, $\varepsilon_0$ is absolute permittivity, $\varepsilon_r$ is the relative permittivity, $\theta$ is the surface area covered of the electrode plate, $g$ is the gap between the plates, and $r$ is the radius of the hemisphere. Therefore

$$C = n\frac{\varepsilon_0\varepsilon_r\pi r^2}{(g-\zeta)} + \frac{\varepsilon_0(\theta - n\pi r^2)}{(g-\zeta)},$$

$$= \frac{\varepsilon_0(\theta + n\pi r^2(\varepsilon_r - 1))}{(g-\zeta)}, \tag{11}$$

Now the sensitivity of the sensor $\lambda$ becomes,

$$\lambda = \frac{\varepsilon_0(\theta + (\varepsilon_r - 1)n\pi r^2)}{P(g-\zeta)}. \tag{12}$$

The radius of the dielectric polymer hemisphere, length and breadth of the electrode, gap between electrode, deflection, and relative permittivity are the parameters that affect the overall sensitivity of the sensor.

## 3. Simulation of TMCPS in Comsol

The A 3D model of the TMCPS includes a diaphragm, mechanical coupler, moving electrode plate, fixed electrode plate and hemisphere shape dielectric polymers and built in the COMSOL Multiphysics simulator as shown in figure 1. The dimension of the various components of the TMCPS is tabulated in table 1 and the necessary material properties of the TMCPS are tabulated in table 2.

**Table 1:** the dimension of the various components of the TMCPS.

| Components | Material | Dimensions | | |
|---|---|---|---|---|
| | | Length | Breath | Thickness or Radius |
| Diaphragm | Gold | 300 µm | 300 µm | 20 µm |
| Mechanical Coupler | $SiO_2$ | 20 µm | 20 µm | 20 µm |
| Electrode Plates | Gold | 300 µm | 300 µm | 20 µm |
| Polymer Dielectric | PMMA | - | - | 40 µm |

**Table 2:** The physical properties of the TMCPS.

| Material | Young's modulus | Poisson's ratio | Relative permittivity |
|---|---|---|---|
| $SiO_2$ | 70 GPa | 0.17 | - |
| Gold | 70 GPa | 0.425 | - |
| PMMA | - | - | 3 |

### 3.1 Simulation Output

The 3D model of the TMCPS is simulated for the applied pressure range of 0.1 MPa to 10.1 MPa with a step size of 1 MPa. Figure 3 shows the deflection output of a TMCPS with 20 µm diaphragm thicknesses at the applied pressure of 10.1 MPa.

From the figure 3 the maximum deflection of the diaphragm occurs at the middle as it was predicted in equation 7. Form the figure 4 output capacitance of the TMCPS using mechanical coupler is highly linear to the applied pressure.

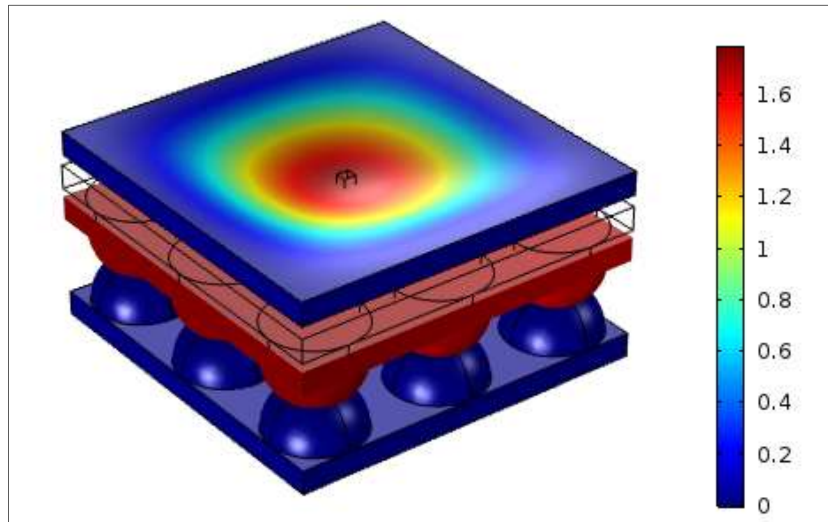


**Fig 1:** Output deflection of the TMCPS at 10.1 MPa.

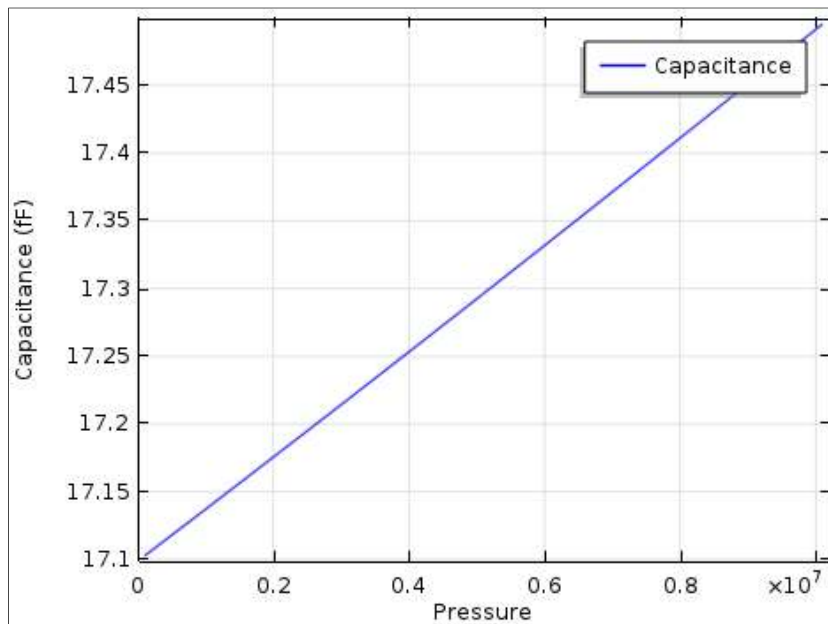


**Fig 2:** Output capacitance of the TMCPS for the applied pressure range from 0.1 to 10.1 MPa.

## 4. Comparative Studies of Simulated and Calculated Values

There Table III lists the simulated and calculated deflection of the diaphragm and output capacitance values for the proposed TMCPS for the applied pressure range from 0.1 MPa to 10.1 MPa with a step size of 1 MPa.

The deflection of the diaphragm is measured at the centre of the diaphragm as the maximum deflection is occurs at the centre and the mechanical coupler is also attached at the centre. The deflection of the diaphragm increases with increase in applied pressure. For the identical input pressures, the simulated and calculated deflection values are quite near to each other.

Again table 3 also listed calculated and simulated values of capacitance for the proposed TMCPS. It can be seen from these data that the output capacitance is in the femto Farad (fF) range. With an increase in applied pressure, the output capacitance values correspondingly rise.

**Table 3:** Simulated vs calculated values for square diaphragm based TMCPS

| Pressure (MPa) | Diaphragm Deflection | | Output Capacitance | |
|---|---|---|---|---|
| | Simulated | Calculated | Simulated | Calculated |
| 0.1 | 0.0174µm | 0.0186µm | 17.1025fF | 17.7623fF |
| 1.1 | 0.1916µm | 0.2046µm | 17.1408fF | 17.7991fF |
| 2.1 | 0.3658µm | 0.3906µm | 17.1793fF | 17.8360fF |
| 3.1 | 0.5398µm | 0.5766µm | 17.2181fF | 17.8731fF |
| 4.1 | 0.7136µm | 0.7625µm | 17.2571fF | 17.9103fF |
| 5.1 | 0.8872µm | 0.9485µm | 17.2963fF | 17.9477fF |
| 6.1 | 1.0611µm | 1.1345µm | 17.3357fF | 17.9853fF |
| 7.1 | 1.2339µm | 1.3205µm | 17.3753fF | 18.0230fF |
| 8.1 | 1.4076µm | 1.5065µm | 17.4152fF | 18.0609fF |
| 9.1 | 1.5791µm | 1.6924µm | 17.4552fF | 18.0989fF |
| 10.1 | 1.7516µm | 1.8784µm | 17.4954fF | 18.1371fF |

Figure 5 depicts the simulated and calculated deflection of the square diaphragm with thickness of 20μm. The deflection of the diaphragm is found to be linear with the input pressure. This deflection is converted into linear displacement by the mechanical coupler. It is observed that the simulated and calculated deflections are very closed. The simulated output values are lower than the calculated output values of the sensor.

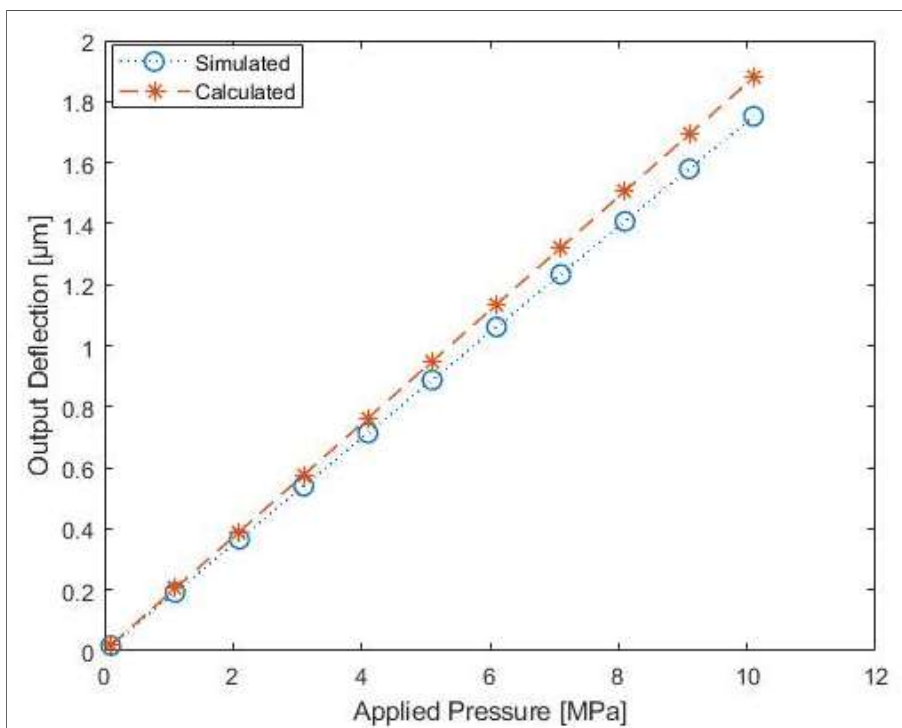


**Fig 5:** Comparison of simulated and calculated values of deflection at the centre of the diaphragm.

Figure 6 depicts the simulated capacitance and calculated capacitance the PMMA-based TMCPS with a diaphragm thickness of 20 μm. The sensor output capacitance is found to be highly linear with the input pressure, which is a desirable property. It can also be shown that the calculated and simulated values are fairly similar. The simulated output values are lower than the calculated output values of the sensor. The slopes or sensitivity of the simulated and calculated values are similar to each others.

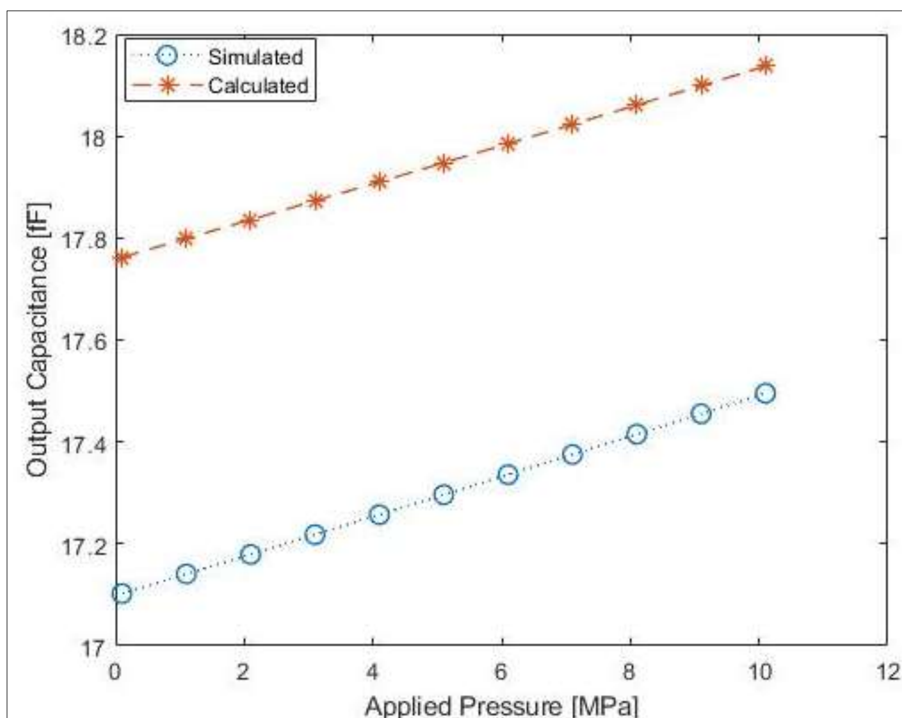


**Fig 6:** Comparisons of simulated and calculated values of capacitance for the designed TMCPS.

## 5. Conclusion

The mathematical modelling and simulation of a TMCPS for detecting and linearization of the out characteristics are the main objectives of this research work. Hemispherical polymer dielectric PMMA is used to enhance the sensitivity of TMCPS as the dielectric constant of PMMA is 3. The design methodology is proposed and can be used in the future

because the simulated and calculated values are near to one another.

As the equations 7, 11, and 12 are validated with the COMSOL multiphysics simulator by comparing the calculated values and simulated values. The physical parameters and mechanical properties of the diaphragm affected the sensitivity of TMCPS. The deflection is inversely related to diaphragm thickness so sensitivity improves when the diaphragm thickness is reduced. The sensitivity of the diaphragm rises as the length of the diaphragm increases. The Young's modulus and Poisson's ratio also affected the sensitivity of the TMCPS.

From equation 11, the gap between the plates is inversely proportional to the sensor's sensitivity. Increases in the area of the electrode plate and the area covered by dielectric polymers will result in higher output capacitances. The relative permittivity of the polymers dielectric increases the output capacitance of the sensors. The mechanical coupler convert the deflection of the diaphragm into linear.

## 6. References


1. Chen D, Cai Y, Huang MC. Customizable Pressure Sensor Array: Design and Evaluation. IEEE Sensors Journal. 2018;18(8):6337-6344.
2. Yang W, Yang Q, Yan R, Zhang W, Yan X, Gao F, *et al*. Dynamic Response of Pressure Sensor With Magnetic Liquids. IEEE Transactions on Applied Superconductivity. 2010;20(6):1860-1863.
3. Li L, Wang L, Qin L, Lv Y. The theoretical model of 1-3-2 piezocomposites. IEEE Transactions on Ultrasonics, Ferroelectrics, and Frequency Control. 2009;56(7):1476-1482.
4. Shu L, Tao X, Feng DD. A New Approach for Readout of Resistive Sensor Arrays for Wearable Electronic Applications. IEEE Sensors Journal. 2015;15(1):442-452.
5. Bakhoum EG, Cheng MHM. High-Sensitivity Inductive Pressure Sensor. IEEE Transactions on Instrumentation and Measurement. 2011;60(8):2960-2966.
6. Houri CG, Talbi A, Viard R, Gallas Q, Garnier E, Molton P, *et al*. Robust thermal microstructure for designing flow sensors and pressure sensors. In Proceedings of the IEEE Sensors; c2017. p. 1-3.
7. Bera SC, Mandal N, Sarkar R. Study of a Pressure Transmitter Using an Improved Inductance Bridge Network and Bourdon Tube as Transducer. IEEE Transactions on Instrumentation and Measurement. 2011;60(4):1453-1460.
8. Luo J, Zhang L, Wu T, Song H, Tang C. Flexible piezoelectric pressure sensor with high sensitivity for electronic skin using near-field electrohydrodynamic direct-writing method. Extreme Mechanics Letters. 2021;48(10):101279.
9. Houri CG, Talbi A, Viard R, Gallas Q, Garnier E, Molton P, *et al*. MEMS high temperature gradient sensor for skin-friction measurements in highly turbulent flows. In Proceedings of the IEEE Sensors; c2019.
10. Alveringh D, Schut TVP, Wiegerink RJ, Sparreboom W, Lötters JC. Resistive pressure sensors integrated with a coriolis mass flow sensor. In Proceedings of the 19th International Conference on Solid-State Sensors, Actuators and Microsystems (TRANSDUCERS); c2017. p. 167-1170
11. Meetei MS, Singh HS, Singh AD, Majumder S. A novel design and optimization for beam bridge piezoelectric pressure sensor. 2020;11(12):2687-2701.
12. Meetei MS, Singh HS. Modelling and Simulation of a Diaphragm based Touch Mode Capacitive Pressure Sensor (DTMCPS). International Journal of Mechanical Engineering. 2021;6(12):2784-2788.
13. Cotton DPJ, Graz IM, Lacour SP. A Multifunctional Capacitive Sensor for Stretchable Electronic Skins. IEEE Sensors Journal. 2009;9(12):2008-2009.
14. Timoshenko SP, Woinowsky-Krieger S. Theory of Plates and Shells. New York: Mc Graw Hill; c1959.
15. Ugural AC. Plates and shells: theory and analysis. Boca Raton, London, New York; c2018.
16. Bao M. Analysis and Design Principles of MEMS Devices. Elsevier Science; c2005.